IEEE Access
Multidisciplinary | Rapid Review | Open Access Journal

Received March 26, 2019, accepted April 23, 2019, date of publication May 24, 2019, date of current version June 7, 2019.

Digital Object Identifier 10.1109/ACCESS.2019.2918784

Variation Pattern Recognition of the BIW OCMM Online Measurement Data Based on LSTM NN

CHANGHUI LIU, KUN CHEN, SUN JIN, AND YUAN QU
State Key Laboratory of Mechanical System and Vibration, Shanghai Jiao Tong University, Shanghai 200240, China

Corresponding author: Sun Jin (leo20702@outlook.com)

This work was supported in part by the Ministry of Industry and Information Technology of China under Grant 17GFBZB02194 and Grant 18GC04246, in part by the National Science and Technology Major Project under Grant 2017-VII-0008-0102, and in part by the China Postdoctoral Science Foundation under Grant 17Z102060069.

ABSTRACT An accurate recognition of a dimensional variation pattern is very important for producing high-quality body-in-white (BIW). The wide application of optical coordination measurement machines (OCMM) in vehicle factory provided massive online dimensional data for the variation pattern recognition. However, the massive serially correlated or autocorrelated and 100% measurement data generated from the OCMM challenge the traditional statistical process control (SPC) technology and the common variation recognition approaches. This paper presents a novel deep-learning method, long short-term memory neural network (LSTM NN), to recognize the variation pattern of the BIW OCMM online measurement data. A comparative study between the backpropagation neural network (BP NN) and the LSTM NN was implemented, and the practicability of the proposed intelligent method was demonstrated by a case study. With the efficient use of time series information, the LSTM NN has a good performance in variation patterns' recognition and high practicability in improving the quality of the BIW.

INDEX TERMS Variation pattern recognition, long short-term memory neural network (LSTM NN), body-in-white (BIW), online measurement data, deep learning.

I. INTRODUCTION

Body-in-white (BIW) is the main component of an automobile, which dimensional accuracy directly affects the quality of the whole vehicle. While the dimensional variation reduction of the BIW is always a tough task for the vehicle factory due to its complex assembly, which involves 100 to 150 sheet metal parts and 80-120 assembly stations [1]. Any deviations introduced by incoming parts or any failures occur at these stations would be finally accumulated to the BIW.

In order to monitor the final quality of BIW, online optical coordination measurement machines (OCMM) are widely applied in the vehicle factory [2]. They are installed at the end of each assembly line and use more than 100 optical laser sensors to measure the key measurement points (MPs) set at the final BIW. With its non-contact, high efficiency and full sample measurement, a tremendous amount of serially correlated and 100% sampled online dimensional data are obtained (approximately 1 min per BIW and 500 vehicles per day). However, the massive dimensional data generated from the OCMM is not fully utilized by the manufacturers. These OCMM data are usually used to recognize the variation patterns only by manual analysis in many vehicle factories [2].

The conventional control charts, as one of the most important statistical process control (SPC) tools for quality control and improvement, has been widely used in the vehicle factory. The effectiveness of using control charts largely depends on the correct recognition for different kinds of variation patterns, which named as control chart pattern (CCP) [3], [4]. Eight types of CCPs are summarized by Gauri [5] and Gauri and Chakraborty [6], and the common variation patterns for BIW are normal (NOR), upward shift (US), downward shift (DS), increasing trend (IT), and decreasing trend (DT). In practice, quality engineers usually use the coordination measurement machine (CMM) to sample the deviation of the BIW and keep the data are uncorrelated. Then the quality monitoring and the CCP recognition can be implemented based on the SPC techniques and their engineering experience. Nevertheless, the serially correlated or autocorrelated 100% measurement data generated from the OCMM challenges the SPC control technologies [7]. The SPC for the BIW OCMM data has the following limitations:

The associate editor coordinating the review of this manuscript and approving it for publication was Naveed Akhtar.

(1) The SPC is a time-consuming procedure for the fast data processing and information extraction in the high rate online measurement system. It is to plot quality observations vs. sample sequences with specific control limits. If there are points exceed control limits or some nonrandom variation patterns happened the process is estimated as out-of-control. The assignable causes for the out-of-control should be identified and removed so that the process is able to back to normal. While reacting to these out-of-control conditions is not easy applying SPC techniques alone.

(2) Control charts are based on the assumption of independent data. However, the BIW OCMM data are a complex time-varying signal with complex correlations at a range of different timescales. The assumption of independent data may not only result in the loss of information of the process which may be quite useful for studying the process and identifying the assignable cause but also lead to high-frequency false alarms, such as alarms indicating process out of control when the process is actually in control.

From the quality control viewpoint, the impact of OCMM data on the quality engineering function is a requirement for a faster and higher accuracy CCP recognition can be implemented so that the feedback loop between the fault diagnosis and corrective action can be closed within a sufficiently small-time frame to avoid or minimize defective products. Therefore, more accurate, effective, automatic and intelligent variation pattern recognition methods are needed to address this challenging problem in the BIW assembly.

Generally, the common CCP recognition approaches can be subsumed under just two broad categories: run-rule-based Expert Systems (ESs) [8] and machine learning methods including the support vector machine (SVM) [9] and artificial neural networks (ANNs) [10]. The comparison of these three methods is summarized in Table 1. According to the comparison, we know that each method has its advantages and disadvantages. Even though the largest problem the ANNs encountered in the modeling process is the requirement for a large amount of training data, whereas it is exactly what online OCMM measurement data can provide in the recognition of dimensional variation pattern of BIW. In order to overcome the corresponding shortcomings of each method, a lot of improvement models have been proposed, especially for the ANNs. However, for its actual application in the recognition of dimensional variation pattern for BIW the ANNs still must face the problem that how to process and utilize the serially correlated or autocorrelated OCMM data effectively.

With the development of deep learning algorithm, a lot of deep artificial neural networks have been proposed and have won numerous contests in pattern recognition [22]. Long Short-Term Memory Neural Network (LSTM NN), as a special recurrent neural network (RNN) structure, is designed to model temporal sequences and their long-term dependencies [23], [24]. In other words, the LSTM NN is very suitable for dealing with the serially correlated or autocorrelated data. It has been successfully applied to various sequence recognition and sequence prediction tasks, such as handwriting recognition [25], [26], large-scale acoustic modeling and vocabulary speech recognition [27]–[29], document analysis and recognition [30], [31], image recognition [32], [33], machine translation [34], traffic speed prediction [35], real-time safety monitoring in the induction motor [36], and so on. To the best of our knowledge, there is no application of LSTM NN in the domain of the variation pattern recognition for the BIW OCMM data.

TABLE 1. Three types of methods to recognize CCPs.

Category	Method	Advantage	Disadvantage	Improvement models
Based on run rules	ESs	Contains information explicitly; Can be modified or updated easily;	No one-to-one correspondence between an abnormal pattern and a running rule; Heavily relying on the experience of engineers;	IntelliSPC [8], Internet-based EPs[11], EPs for on-line detection[12]
Based on machine learning	SVM	Good generalization ability in small sample;	Hard to select correct kernel functions and optimize its corresponding parameters;	MCSVM[13], PS-SVM([14], DAGSVM[15], BTSVM[16]
	ANNs	Non-parametric; Non-linear; Adaptive learning;	Big training data requirement;	BP[17], MLP [5], LVQ[18], K-MICA based ANNs[19], COA-RBFNN[20], PSO-BP[21]

In order to address the drawbacks of the conventional ANNs brought by the complex time-varying and serially correlated or autocorrelated data, we explore LSTM NN architectures for the variation pattern recognition of the large-scale BIW OCMM online measurement data. Based on the discussion above, the contribution of this paper mainly contains: (1) a novel recurrent neural network architecture: Long Short-Term Memory Neural Network, is developed to capture the correlation or autocorrelation OCMM online measurement data for the variation pattern recognition of the BIW; (2) a comparative study between the Backpropagation Neural Network (BP NN) and the LSTM NN is implemented to provide a general guideline for selecting different ANN structures for the variation pattern recognition of the BIW; (3) an actual case is studied to demonstrate the practicability of the proposed intelligent method.

The remainder of the paper is organized as follows. In Section 2, an automatic and intelligent method to recognize the variation pattern of the BIW based on the LSTM NN is

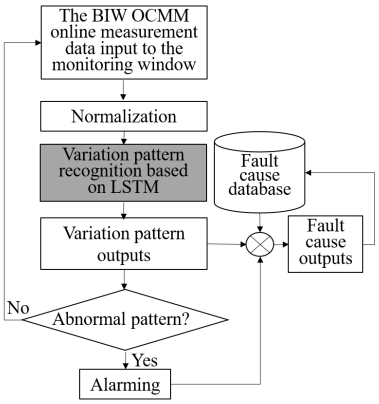

FIGURE 1. An overview of the proposed intelligent method based on LSTM NN.

developed. Based on the proposed method, the experiment is carried out to verify the recognition accuracy, followed by a comparative study between the BP NN and the LSTM NN in Section 3. In Section 4, a case study will be implemented to demonstrate the practicability of the proposed intelligent method in the variation pattern recognition of the BIW. Finally, the conclusions and some future works are discussed in Section 5.

II. METHODOLOGIES

A. OVER REVIEW OF THE INTELLIGENT METHOD

In this paper, an automatic and intelligent system for the variation pattern recognition of the BIW is proposed (see Fig. 1). First, the BIW OCMM online measurement data are input to the monitoring window, followed by the normalization preprocessing. Then a recognition process for the variation pattern based on the trained LSTM NN is proposed to implement. If the variation pattern output is an abnormal pattern, the alarm system will trigger the alarm and the quality engineer will diagnose the corresponding fault cause according to the type of abnormal pattern and the fault cause database. Otherwise, new BIW OCMM online measurement data will be input the monitoring window.

B. LSTM NN MODEL FOR VARIATION PATTERN RECOGNITION

In order to overcome the disadvantages of the traditional ANNs in dealing with the complex time-varying data, LSTM NN is developed in this paper to recognize the variation pattern of the serially correlated or autocorrelated OCMM online measurement data. The LSTM NN consists of one input layer, one recurrent hidden layer, and one output layer. The biggest structural difference from the traditional ANNs is that there is a set of interrelated recurrent subnetworks, named basic memory block, in the hidden layer. The memory block is controlled by some special adaptive gating units to save, write, and read the information. These gate units are essentially logical units which usually contain sigmoid functions and point multiplication operations and can selectively pass through information.

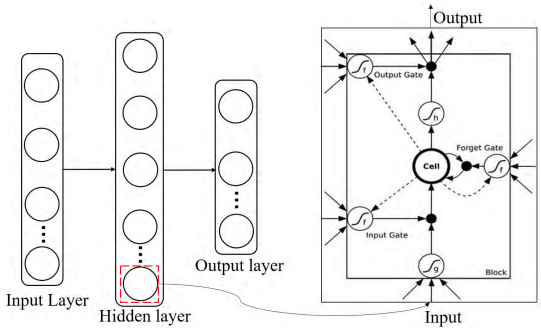

FIGURE 2. The architecture of LSTM NN.

Figure 2 shows the basic architecture of the LSTM NN. There are three nonlinear gate units that responsible for activation. The input and output data are controlled by the input gate and the output gate respectively. The forget gate is added to prevent the internal cell values growing without bound. Three black nodes are directly connected to the corresponding activation functions. The core of the memory cell is a recurrently self-connected linear unit-Constant Error Carousel (CEC), which represents the memory of the neuron state and records the state by adjusting the parameter state. According to the state of CEC, the multiplication gates can learn to open and close, so the LSTM NN solves the problem of vanishing errors by keeping the network error constant. The dashed line represents the weight connection of the node to each gate at the previous moment, and the weight value of the other connections is a fixed constant of 1. And the only output of the neural network to the next time step is the transmission at the output gate.

Let w_{ij} denote the connection weight between unit i and unit j of the LSTM NN, a_j^t and b_j^t denote the input and output of the unit j at time t. The input gate, forget gate and output gate are respectively corresponding to n, φ and ω. I, H and K represent the neurons number of the input layer, the hidden layer, and the output layer, respectively. C denotes the number of the memory cell. Then the input of the memory cell n is:

$$a_n^t = \sum_{i=1}^{I} w_{in} x_i^t + \sum_{h=1}^{H} w_{hn} b_h^{t-1} + \sum_{c=1}^{C} w_{cn} s_c^{t-1} \tag{1}$$

where x_i^t denotes the value of unit i at time t, b_h^{t-1} denotes the output of unit h at time $t-1$, s_c represents the state of the memory unit.

In the memory unit of LSTM NN, only the previous moment output b_h of the forget gate will be transmitted to this unit. The output of the forget gate is:

$$b_\varphi^t = \sum_{i}^{I} w_{i\varphi} x_i^t + \sum_{h}^{H} w_{h\varphi} b_h^{t-1} + \sum_{c}^{C} w_{c\varphi} s_c^{t-1} \tag{2}$$

The input of the memory unit is:

$$a_c^t = \sum_{i''}^{I} w_{ic} x_i^t + \sum_{h}^{H} w_{hc} b_h^{t-1} \tag{3}$$

The state of the memory unit is:

$$s_c^t = b_\varphi t s_c^{t-1} + b_n^t g\left(a_c^t\right) \tag{4}$$

The input of the output gate is:

$$a_\omega^t = \sum_{i=1}^{I} w_{i\omega} x_i^i + \sum_{h=1}^{H} w_{h\omega} b_h^{t-1} + \sum_{c=1}^{C} w_{c\omega} s_c^t \tag{5}$$

The activation function can be denoted as:

$$b_k^t = f(a_k^t) \tag{6}$$

where k can be written as n, φ and ω, denoting the input gate, forget gate and output gate, respectively.

The output of the node corresponding to Eq. (3) is controlled by output gate, the output is also the input to the entire memory unit at the next moment. It can be represented as:

$$b_c^t = b_\omega^t h(s_c^t) \tag{7}$$

The activation function of the output gate is generally the logistic function or the *softmax* function. In order to facilitate the reverse transmission of the representation error, the following intermediate variables are defined by the chain rule:

$$\begin{aligned}\varepsilon_c^t &= \frac{\partial L}{\partial b_c^t} = \sum_{k=1}^{K} \frac{\partial L \partial a_k^t}{\partial a_k^t \partial b_c^t} + \sum_{h=1}^{H} \frac{\partial L \partial a_h^t}{\partial a_h^t \partial b_c^t} \\ &= \sum_{k=1}^{K} w_{ck} \delta_k^t + \sum_{h=1}^{H} w_{ch} \delta_h^{t+1}\end{aligned} \tag{8}$$

$$\begin{aligned}\varepsilon_s^t &= \frac{\partial L}{\partial s_c^t} \\ &= b_\omega^t h^{'}\left(s_c^t\right) \varepsilon_c^t + b_\varphi^{t+1} \varepsilon_s^{t+1} + w_{c\omega} \delta_\omega^t + w_{cn} \delta_n^{t+1} \\ &\quad + w_{c\varphi} \delta_\varphi^{t+1}\end{aligned} \tag{9}$$

where L denotes the loss function. It acts sequentially on the memory cell, the forget gate and the input gate:

$$\delta_c^t = \frac{\partial L}{\partial a_c^t} = \frac{\partial L}{\partial s_c^t} \frac{\partial s_c^t}{\partial g\left(a_c^t\right)} \frac{\partial g\left(a_c^t\right)}{\partial a_c^t} = \varepsilon_c^t b_n^t g^{'}(a_c^t) \tag{10}$$

$$\delta_\varphi^t = \frac{\partial L}{\partial a_\varphi^t} = \sum_{c=1}^{C} \frac{\partial L}{\partial s_c^t} \frac{\partial s_c^t}{\partial b_\varphi^t} \frac{\partial b_\varphi^t}{\partial a_\varphi^t} = f^{'}(a_\varphi^t) \sum_{c=1}^{C} s_c^{t-1} \varepsilon_s^t \tag{11}$$

$$\delta_n^t = \frac{\partial L}{\partial a_n^t} = \sum_{c=1}^{C} \frac{\partial L}{\partial s_c^t} \frac{\partial s_c^t}{\partial b_n^t} \frac{\partial b_n^t}{\partial a_n^t} = f^t(a_n^t) \sum_{c=1}^{C} g(a_n^{t-1}) \varepsilon_s^t \tag{12}$$

The partial derivative of weight w_{ij} is obtained by using loss function:

$$\frac{\partial L}{\partial w_{ij}} = \sum_t \frac{\partial L \partial a_j^t}{\partial a_j^t \partial w_{ij}} = \sum_t \delta_j^t b_i^t \tag{13}$$

The value of initial weights has a great influence on the training results of the LSTM NN model. The values of initial weights were calculated according to the activation function of the network nodes, the number of input and output nodes per layer. The parameter initialization formulas are as follows:

$$\begin{aligned}&\tanh: W \sim Uniform \\ &\times \left(-\frac{\sqrt{6}}{\sqrt{fan_{in} + fan_{out}}}, \frac{\sqrt{6}}{\sqrt{fan_{in} + fan_{out}}}\right)\end{aligned} \tag{14}$$

$$\begin{aligned}&sigmoid: W \sim Uniform \\ &\times \left(-4^* \frac{\sqrt{6}}{\sqrt{fan_{in} + fan_{out}}}, 4^* \frac{\sqrt{6}}{\sqrt{fan_{in} + fan_{out}}}\right)\end{aligned} \tag{15}$$

where fan_{in} and fan_{out} represent the number of the input and the number of the output for the network nodes, respectively. *Uniform* represents the uniform distribution. The value of weights can be selected in its interval.

TABLE 2. Experiment environment.

Item	Environment
Development language	Python
Library	*Keras*
Disk capacity	1T
RAM	20G
CPU	Intel (R) Core (TM) i7-4770 CPU 3.4GHz
OS	Windows Server 2008 R2 Enterprise 64bit

III. EXPERIMENT

A. EXPERIMENT ENVIRONMENT

In this paper, the experiment environment of LSTM NN is based on Python 3.6.0-0. Anaconda was used to write the program. It has a powerful and convenient function package management and environment management ability. A deep learning library, *Keras*, was applicated to construct the LSTM NN for parallel computing. The specific experiment environment is shown in Table 2.

B. DATA PREPROCESSING

In this section, the actual OCMM online measurement data from July 2017 to July 2018 for a specific kind of BIW produced in a vehicle factory were collected and 1000 groups for each pattern including NOR, IT, DT, US, and DS were summarized. The length of data for each group was 60, which means each pattern was taken as a time series of 60 data points. Monte Carlo simulation method was used to generate similar data. The simulation equations for different various patterns were shown in Table 3. The values of parameters were calculated based on the actual OCMM online measurement data.

Based on these simulation equations, 4000 groups data for each variation pattern were generated so that there were

TABLE 3. Variation pattern simulation equations.

CCPs	Simulation equations	Parameters
NOR	$x(t)=\mu+\sigma_{noi}r(t)$	μ=0 : the mean of the sample, t : the discrete time $r(t)\sim N(0,1)$: a random number generating function σ_{noi}=0.5 : the standard deviation of system noise $s\in[0.8,2.3]$: the magnitude of the shift b=0 or 1 : the shift position, $k\in[0.05,0.15]$: the gradient
IT	$x(t)=\mu+\sigma_{noi}r(t)+kt$	
DT	$x(t)=\mu+\sigma_{noi}r(t)$-$kt$	
US	$x(t)=\mu+\sigma_{noi}r(t)+bs$	
DS	$x(t)=\mu+\sigma_{noi}r(t)$-$bs$	

5000 groups data for each variation pattern including the actual data groups. These 5000 groups data were randomly distributed. After the min-max normalization (MMN) process was carried out, the data preprocessing was finished.

C. CONTRAST EXPERIMENT

1) THE SIMULATION OF LSTM NN

In this experiment, the LSTM NN was constructed according to reference [37]. There were one hidden layer and one output layer, and their corresponding numbers of units were 50 and 5, respectively. The 5 units of the output layer denote five different patterns including NOR, IT, DT, US, and DS. The *Sequential*, *Dense* and*Activation* in the*Keras* framework proceeded. The *Softmax* function acted as the activation function, and the corresponding *categorical_crossentropy* function was selected as the loss function. According to reference [38], the advantage of matching the activation function with the loss function is that the derivative of the loss function of each output unit to the input is equal to the difference between the actual output and the ideal output in the process of error reverse transfer. The index list *metrics* selects the default accuracy. The optimizer parameter was set as *RMSprop*. The batch size was set to 20. The number of iterations was 50. The initialization of the LSTM NN is summarized in Table 4. In the training and testing process, 70% of training samples and 30% of test samples were randomly selected from the whole data set, including 1000 groups of actual data and 4000 groups of simulation data for each pattern.

2) THE SIMULATION OF BP NN

In order to verify the superiority of the LSTM NN in variation pattern recognition of the serially correlated or autocorrelated OCMM online measurement data, a similar BP NN architecture in reference [39] was also applied. There were 2 hidden layers and the neuron number for the 1st and 2nd hidden layer was 10 and 7, respectively. The combination of statistical features (including mean, standard deviation, mean square value, skewness, and kurtosis [40]) and shape features (including SB, AASL, SRANGE, and REAE [6]) was chosen as the input. The initialization of BP NN is summarized in Table 5. Then the training and the testing of the BP NN were performed using the data set mentioned above.

TABLE 4. LSTM NN initialization.

Learning algorithm	Activation function	Loss function	Batch size	Iteration
RMSprop	*Softmax*	*categorical_crossentropy*	20	50

TABLE 5. BP NN initialization.

Learning algorithm	Activation function for the hidden layer	Activation function for the output layer	Learning rate	Minimum error	Training steps
trainlm	*logsig*	*purelin*	0.05	0.01	2000

TABLE 6. Comparison of recognition performance between LSTM NN and BP NN.

Model	Average recognition accuracy (%)		Mean percentage for confusion				
			IT	DT	US	DS	NOR
BP	94.72	IT	91.50	0.00	8.50	0.00	0.00
		DT	0.00	95.20	0.00	4.80	0.00
		US	6.50	0.00	93.50	0.00	0.00
		DS	0.00	6.60	0.00	93.40	0.00
		NOR	0.00	0.00	0.00	0.00	100.0
LSTM	99.78	IT	99.90	0.00	0.10	0.00	0.00
		DT	0.00	100.0	0.00	0.00	0.00
		US	0.30	0.00	99.70	0.00	0.00
		DS	0.00	0.70	0.00	99.30	0.00
		NOR	0.00	0.00	0.00	0.00	100.0

D. RESULT ANALYSIS AND COMPARISON

In order to prove the superiority of the LSTM NN model in identifying abnormal deviation pattern of BIW OCMM online measurement data, the LSTM NN model was established according to the above procedure. Finally, compared with the traditional BP NN, the recognition accuracy is shown in Table 6. It can be found that, with its efficient use of time series information of online measurement data, the overall average recognition accuracy for the five quality patterns can reach 99.78% by using LSTM NN, which is 5.34% higher than that of BP NN. Moreover, the recognition accuracy of LSTM for each variation pattern is more consistent. Especially, its recognition accuracy of DT and that of NOR can reach 100%. It is fully demonstrated that the LSTM NN can effectively eliminate the confusion between different patterns and accurately identify all kinds of abnormal variation patterns of BIW based on the online measurement data.

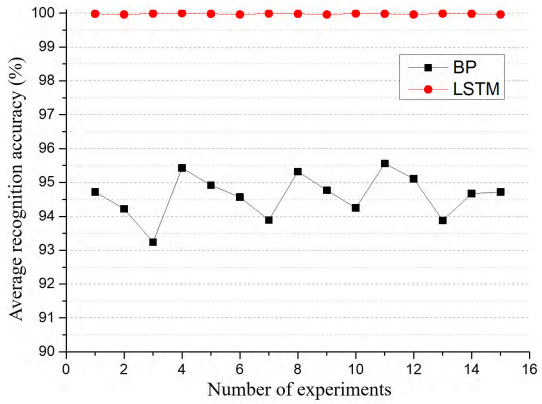

FIGURE 3. Average recognition accuracy of 15 repeated experiments.

TABLE 7. The statistics of the 15 experimental recognition results.

Model	The mean value of average recognition accuracy (%)	The standard deviation of average recognition accuracy
BP	94.618	0.64
LSTM	99.977	0.01

In order to evaluate the robustness of recognition ability, 15 repeated experiments were implemented. The average recognition accuracy of LSTM NN and that of BP NN are shown in Fig. 3. The recognition accuracy of LSTM NN is higher and more stable than that of BP NN because the average recognition accuracies of LSTM NN in these 15 repeated experiments closed to 100%, while that of BP NN in these 15 repeated experiments varied in the range of 93.89% and 95.56%. The same result can also be summarized according to Table 7. In Table 7, the mean value of average recognition accuracy for these 15 repeated experiments is calculated and make a comparison between LSTM NN and BP NN. The mean value of average recognition accuracy of LSTM NN and BP NN is 99.98% and 94.62% respectively, which means the average recognition accuracy of LSTM NN is higher than that of BP NN. The standard deviation of average recognition accuracy of LSTM NN and BP NN are 0.01 and 0.64 respectively, which means the performance of LSTM NN is more stable than that of BP NN.

IV. CASE STUDY

The shape of taillight has said goodbye to the simple plane and straight-line structure. The complex surface and curve of taillights make the matching gap control among the taillight, the out plate of the side wall and the welded part of D-pillar in the assembly process to be one of the most difficult works in the of vehicle quality control. So, it is necessary to monitor the taillight installation area in the actual BIW assembly process and some MPs are set in this area (see Fig. 4).

The actual OCMM online measurement data of MPs in the taillight area on March 4, 2018, were selected, which was a total of 500 vehicle samples. The proposed intelligent method was used to recognize the variation pattern. The monitoring window for data number was 60 and the trained LSTM NN in

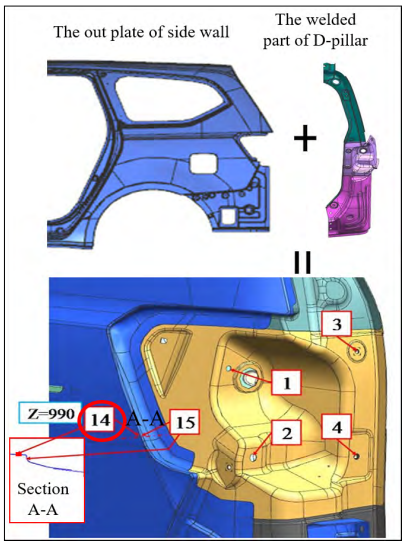

FIGURE 4. The set of MPs in the taillight installation area.

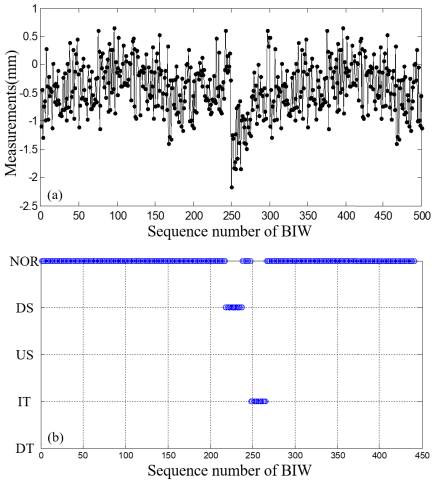

FIGURE 5. NO.14 MP (a) the measurements (b) the variation pattern recognition.

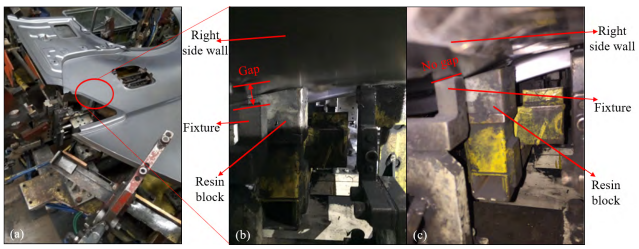

FIGURE 6. The fault cause for the abnormal pattern (a) fault section (b) the cause for the DS (c) the cause for the IT.

the above experiment was applied. When the data were read, the recognition process was performed as shown in Fig.1. Taking the y-direction measurement data of the NO.14 MP as an example, all the measurement value of NO.14 MP in the y-direction are shown in Fig. 5(a) and the corresponding recognition results were shown in Fig. 5(b).

From Fig. 5(a) we know that when the monitoring window moved to the 218th sample a DS happened, and the alarm system triggered the alarm. The quality engineer responded in

time and the diagnosis was carried out based on the fault cause database and a site investigation for the assembly process of the right-side wall was also conducted (see Fig. 6(a)). The final diagnosis result was that the resin block of the elevator mechanism in the side wall assembly line and the outer plate of the side wall interfered with each other, which resulted in a 2-3mm gap between the positioning surface of the fixture and the side wall (see Fig. 6(b)). So, the right-side wall of the taillight area will jump in a short period of time.

When the monitoring window moved to the 248th sample, the abnormal variation pattern was identified as a UT and continued to the 265th sample (see Fig. 5(b)). This was due to the continuous wear of the resin block in contact with the outer plate of the side wall after interference. The stiffness of the resin block was relatively small, the wear process was very rapid, which led to a UT from the 248th to the 265th sample.

When the monitoring window moved to the 266th sample, the output result of recognition was a NOR, which indicated that the assembly process was in normal condition again. At this time, the resin block was worn to a certain extent, removing its own interference, and eliminating the gap between the positioning surface of the fixture and the side wall (see Fig. 6(c)). The results of recognition were in good agreement with the cause of the investigation.

V. CONCLUSION

The dimensional variation pattern recognition for BIW plays a very important role in the quality improvement of the automotive body assembly. The wide application of OCMM provided a tremendous amount of online dimensional data. However, the massive serially correlated or autocorrelated and 100% measurement data generated from the OCMM challenges the traditional SPC technology and the common CCP recognition approaches. In this paper, we explore the LSTM NN for the variation pattern recognition of the large-scale OCMM online measurement data. In order to validate the effectiveness of the proposed LSTM NN, 1-year actual OCMM online measurement data for a specific kind of BIW produced in a vehicle factory were collected and a comparative experiment between the BP NN and the LSTM NN for variation pattern recognition is implemented based on these data. In addition, a case of the variation pattern recognition for an MP set in the taillight installation area was studied. According to the result analysis of the experiment and the case study, several useful findings can be summarized:

1) The LSTM NN can effectively eliminate the confusion between different patterns and accurately identify all kinds of abnormal variation patterns of the BIW OCMM online measurement data. With the efficient use of time series information, the LSTM NN has a higher overall average recognition accuracy for the five variation patterns, which can reach 99.78%.
2) The LSTM NN has a good robustness in the variation recognition of the BIW OCMM online measurement data. The average recognition accuracies of LSTM NN in 15 repeated experiments are close to 100%, and the corresponding standard deviation of average recognition accuracy of LSTM NN is just 0.01, which means it is more stable than that of BP NN.
3) The LSTM NN has a high practicability in improving the quality of BIW. A case study reveals that the intelligent system based on the LSTM NN can not only recognize the abnormal variation patterns with high accuracy but also help the quality engineer to improve the efficiency and the accuracy of fault diagnoses based on the fault cause database.

Even though this paper mainly focuses on the automatic, intelligent and accurate variation pattern recognition method development for the BIW so that it can help the vehicle manufacturers make a full use of the OCMM online measurement data and improve the quality of BIW, the method proposed in this paper can also be used in the quality variation pattern recognition of the online detection data for other products. In this paper, in order to demonstrate the variation recognition accuracy and the practicability of the proposed method, a simple case with one-dimensional data was studied. While the fault diagnoses of dimensional variation in the BIW assembly process is a complex issue, future work can be conducted by considering the correlation between different MPs and using the massive multivariate online measurement data to develop an intelligent fault diagnose method based on the LSTM NN.

REFERENCES

[1] J. Shi, *Stream of Variation Modeling and Analysis for Multistage Manufacturing Processes*. Boca Raton, FL, USA: CRC Press, 2006.

[2] H. Wang, G. Chen, and P. Zhu, "BIW assembly quality evaluation with variation of OCMM data and data-splitting error estimation," *Int. J. Adv. Manuf. Technol.*, vol. 24, nos. 11–12, pp. 830–833, 2004.

[3] J. Chen and Y. Liang, "Development of fuzzy logic-based statistical process control chart pattern recognition system," *Int. J. Adv. Manuf. Technol.*, vol. 86, nos. 1–4, pp. 1011–1026, 2016.

[4] J. Wang, A. K. Kochhar, and R. G. Hannam, "Pattern recognition for statistical process control charts," *Int. J. Adv. Manuf. Technol.*, vol. 14, no. 2, pp. 99–109, 1998.

[5] S. K. Gauri, "Control chart pattern recognition using feature-based learning vector quantization," *Int. J. Adv. Manuf. Technol.*, vol. 48, nos. 9–12, pp. 1061–1073, 2010.

[6] S. K. Gauri and S. Chakraborty, "Recognition of control chart patterns using improved selection of features," *Comput. Ind. Eng.*, vol. 56, no. 4, pp. 1577–1588, 2009.

[7] S. Hu, "Impact of 100% measurement data on statistical process control (SPC) in automobile body assembly," Ph.D. dissertation, Univ. Michigan, Ann Arbor, MI, USA, 1990.

[8] R.-S. Guh, J. D. T. Tannock, and C. O'Brien, "IntelliSPC: A hybrid intelligent tool for on-line economical statistical process control," *Expert Syst. Appl.*, vol. 17, no. 3, pp. 195–212, 1999.

[9] C.-J. Lu, Y. E. Shao, and C.-C. Li, "Recognition of concurrent control chart patterns by integrating ICA and SVM," *Appl. Math. Inf. Sci.*, vol. 8, no. 2, p. 681, 2014.

[10] S. K. Gauri and S. Chakraborty, "Improved recognition of control chart patterns using artificial neural networks," *Int. J. Adv. Manuf. Technol.*, vol. 36, nos. 11–12, pp. 1191–1201, 2008.

[11] R. Grove, "Internet-based expert systems," *Expert Syst.*, vol. 17, no. 3, pp. 129–135, 2000.

[12] M. Bag, S. K. Gauri, and S. Chakraborty, "An expert system for control chart pattern recognition," *Int. J. Adv. Manuf. Technol.*, vol. 62, nos. 1–4, pp. 291–301, 2012.

[13] V. Ranaee and A. Ebrahimzadeh, "Control chart pattern recognition using a novel hybrid intelligent method," *Appl. Soft Comput.*, vol. 11, no. 2, pp. 2676–2686, 2011.

[14] S. Du, J. Lv, and L. Xi, "On-line classifying process mean shifts in multivariate control charts based on multiclass support vector machines," *Int. J. Prod. Res.*, vol. 50, no. 22, pp. 6288–6310, 2012.
[15] S. Wang, M. Yang, S. Du, J. Yang, B. Liu, J. M. Gorriz, J. Ramírez, T.-F. Yuan, and Y. Zhang, "Wavelet entropy and directed acyclic graph support vector machine for detection of patients with unilateral hearing loss in MRI scanning," *Frontiers Comput. Neurosci.*, vol. 10, p. 106, Oct. 2016.
[16] C. Wu, F. Liu, and B. Zhu, "Control chart pattern recognition using an integrated model based on binary-tree support vector machine," *Int. J. Prod. Res.*, vol. 53, no. 7, pp. 2026–2040, 2015.
[17] C.-S. Cheng, "A neural network approach for the analysis of control chart patterns," *Int. J. Prod. Res.*, vol. 35, no. 3, pp. 667–697, 1997.
[18] N. Gu, Z. Cao, L. Xie, D. Creighton, M. Tan, and S. Nahavandi, "Identification of concurrent control chart patterns with singular spectrum analysis and learning vector quantization," *J. Intell. Manuf.*, vol. 24, no. 6, pp. 1241–1252, 2013.
[19] A. Ebrahimzadeh, J. Addeh, and Z. Rahmani, "Control chart pattern recognition using K-MICA clustering and neural networks," *ISA Trans.*, vol. 51, no. 1, pp. 111–119, Jan. 2012.
[20] J. Addeh, A. Ebrahimzadeh, M. Azarbad, and V. Ranaee, "Statistical process control using optimized neural networks: A case study," *ISA Trans.*, vol. 53, no. 5, pp. 1489–1499, 2014.
[21] J. Cao, H. Cui, H. Shi, and L. Jiao, "Big data: A parallel particle swarm optimization-back-propagation neural network algorithm based on MapReduce," *PLoS ONE*, vol. 11, no. 6, 2016, Art. no. e0157551.
[22] J. Schmidhuber, "Deep learning in neural networks: An overview," *Neural Netw.*, vol. 61, pp. 85–117, Jan. 2015.
[23] F. A. Gers, J. Schmidhuber, and F. Cummins, "Learning to forget: Continual prediction with LSTM," in *Proc. 9th Int. Conf. Artif. Neural Netw. ICANN*, 1999, pp. 850–855.
[24] S. Hochreiter and J. Schmidhuber, "Long short-term memory," *Neural Comput.*, vol. 9, no. 8, pp. 1735–1780, 1997.
[25] A. Graves and J. Schmidhuber, "Offline handwriting recognition with multidimensional recurrent neural networks," in *Proc. Adv. Neural Inf. Process. Syst.*, 2008, pp. 545–552.
[26] A. Graves, M. Liwicki, S. Fernández, R. Bertolami, H. Bunke, and J. Schmidhuber, "A novel connectionist system for unconstrained handwriting recognition," *IEEE Trans. Pattern Anal. Mach. Intell.*, vol. 31, no. 5, pp. 855–868, May 2009.
[27] K. Chen and Q. Huo, "Training deep bidirectional LSTM acoustic model for LVCSR by a context-sensitive-chunk BPTT approach," *IEEE/ACM Trans. Audio, Speech, Language Process.*, vol. 24, no. 7, pp. 1185–1193, Jul. 2016.
[28] H. Zen and H. Sak, "Unidirectional long short-term memory recurrent neural network with recurrent output layer for low-latency speech synthesis," in *Proc. IEEE Int. Conf. Acoust., Speech Signal Process. (ICASSP)*, Apr. 2015, pp. 4470–4474.
[29] H. Sak, A. Senior, and F. Beaufays, "Long short-term memory recurrent neural network architectures for large scale acoustic modeling," in *Proc. 15th Annu. Conf. Int. Speech Commun. Assoc.*, 2014, pp. 338–342.
[30] H. Palangi, L. Deng, Y. Shen, J. Gao, X. He, J. Chen, X. Song, and R. Ward, "Deep sentence embedding using long short-term memory networks: Analysis and application to information retrieval," *IEEE/ACM Trans. Audio, Speech, Language Process.*, vol. 24, no. 4, pp. 694–707, Apr. 2016.
[31] S. Ghosh, O. Vinyals, B. Strope, S. Roy, T. Dean, and L. Heck, "Contextual LSTM (CLSTM) models for Large scale NLP tasks," 2016, *arXiv:1602.06291*, [Online]. Available: https://arxiv.org/abs/1602.06291
[32] L. Wang, Y. Gao, F. Shi, G. Li, J. H. Gilmore, W. Lin, and D. Shen, "LINKS: Learning-based multi-source integration framework for segmentation of infant brain images," *NeuroImage*, vol. 108, pp. 160–172, Mar. 2015.
[33] M. F. Stollenga, W. Byeon, M. Liwicki, and J. Schmidhuber, "Parallel multi-dimensional LSTM, with application to fast biomedical volumetric image segmentation," in *Proc. Adv. Neural Inf. Process. Syst.*, 2015, pp. 2998–3006.
[34] I. Sutskever, O. Vinyals, and Q. V. Le, "Sequence to sequence learning with neural networks," in *Proc. Adv. Neural Inf. Process. Syst.*, 2014, pp. 3104–3112.
[35] X. Ma, Z. Tao, Y. Wang, H. Yu, and Y. Wang, "Long short-term memory neural network for traffic speed prediction using remote microwave sensor data," *Transp. Res. C, Emerg. Technol.*, vol. 54, pp. 187–197, May 2015.
[36] A. Kerboua, A. Metatla, R. Kelaiaia, and M. Batouche, "Real-time safety monitoring in the induction motor using deep hierarchic long short-term memory," *Int. J. Adv. Manuf. Technol.*, vol. 99, nos. 9–12, pp. 2245–2255, 2018.
[37] B. Bakker, "Reinforcement learning with long short-term memory," in *Proc. Adv. Neural Inf. Process. Syst.*, 2002, pp. s1475–1482.
[38] N. M. Nasrabadi, "Pattern recognition and machine learning," *J. Electron. Imag.*, vol. 16, no. 4, 2007, Art. no. 049901.
[39] V. Ranaee and A. Ebrahimzadeh, "Control chart pattern recognition using neural networks and efficient features: A comparative study," *Pattern Anal. Appl.*, vol. 16, no. 3, pp. 321–332, 2013.
[40] A. Hassan, M. S. N. Baksh, A. M. Shaharoun, and H. Jamaluddin, "Improved SPC chart pattern recognition using statistical features," *Int. J. Prod. Res.*, vol. 41, no. 7, pp. 1587–1603, 2003.

CHANGHUI LIU received the B.Sc. degree in mechanical engineering from Hunan University, Changsha, China, in 2010, and the Ph.D. degree from Shanghai Jiao Tong University, Shanghai, China, in 2016.

From 2016 to 2018, he was a Postdoctoral with the Shanghai Key Laboratory of Digital Manufacture for Thin-walled Structures, School of Mechanical Engineering, Institute of Automobile Engineering, Shanghai Jiao Tong University. He is currently a Visiting Research Associate with the H. Milton Stewart School of Industrial and Systems Engineering, Georgia Institute of Technology, Atlanta, GA, USA. His primary research interests include data mining, machine learning, and quality control.

KUN CHEN received the B.Sc. degree in mechanical engineering from Sichuan University, Chengdu, China, in 2015. He is currently pursuing the Ph.D. degree with the Shanghai Key Laboratory of Digital Manufacture for Thin-walled Structures, School of Mechanical Engineering, Institute of Automobile Engineering, Shanghai Jiao Tong University, Shanghai, China. His primary research interests include assembly automation and tolerance analysis based on the driven data.

SUN JIN received the B.Sc. and M.Sc. degrees in mechanical engineering from Hunan University, Changsha, China, in 1995 and 1998, respectively, and the Ph.D. degree in mechanical engineering from Shanghai Jiao Tong University, Shanghai, China, in 2001.

He is currently a Professor with the Department of Mechanical Engineering, Shanghai Jiao Tong University. His current research interests include data analysis, fault diagnosis, manufacturing quality control, assembly technology development, and industrial applications.

Dr. Jin received the Shanghai Technological Invention Award First Prize, the New Technologies and New Methods of the Variation Control for Complicated Sheet Metal Product Design, in 2008, the Ministry of Education, National Science and Technology Progress Award nomination, the Data-Driven Manufacturing Quality Control System for Multi-Species Scale of Customized Products, in 2005, and the Shanghai Science and Technology Progress Award, the Sheet Metal Stamping Quality Control Base on Numerical Simulation, in 2001.

YUAN QU received the B.S. degree in mechanical engineering from the Wuhan University of Technology, Wuhan, China, in 2014, and the M.Sc. degree in mechanical engineering from Shanghai Jiao Tong University, Shanghai, China, in 2017.

He is currently a Junior Researcher from Huawei Technologies Co., Ltd. His current research interests include data mining, assembly tolerance analysis, and quality control.